

The Influence of Microstructure and Stress State on the Service Performance of TiN Coatings Deposited by Dual-stage HIPIMS

Hao Juan^{1,2}, Wang Baichuan¹, Ding Yuhang¹, Yang Chao¹, Jiang Bailing¹, Wang Ziyi¹, Wang Dongcheng²

¹ School of Materials Science and Engineering, Xi'an University of Technology, Xi'an 710048, China; ² Jiashan Xinhai Precision Casting Co., Ltd., Jiashan 314105, China

Abstract: This study utilized a novel dual stage HIPIMS technology to prepare TiN coatings under different deposition time conditions, and analyzed the effects of microstructure and stress state at different growth stages of the coatings on the mechanical, tribological, and corrosion resistance performance of the coatings. The results showed that as the deposition time increased from 30 minutes to 120 minutes, the surface structure of TiN coating exhibited a round cell structure with tightly doped small and large particles, maintaining a deposition crystallization growth atomic stacking thickening mechanism. When the deposition time increases from 90 minutes to 120 minutes, the coating thickness increases from 3884nm to 4456 nm. The stress state of the coating undergoes a compression tension transition. When the deposition time is 90 minutes, the TiN coating structure is dense and the compressive stress is relatively small, with a compressive stress of -0.54 GPa. The coating has high hardness and elastic modulus, which are 27.5 GPa and 340.2 GPa, respectively. Meanwhile, the coating has good tribological and corrosion resistance properties, with an average friction coefficient of 0.52 and minimum wear rate of 1.68×10^{-4} g/s, minimum corrosion current density of $1.0632 \times 10^{-8} \text{ A} \cdot \text{cm}^{-2}$, minimum corrosion rate of $5.5226 \times 10^{-5} \text{ mm} \cdot \text{A}^{-1}$.

Key words: dual-stage HIPIMS; TiN coatings; stress; service performance

Transition metal nitride hard coatings (such as TiN) are widely used in many industries, especially precision instruments and devices, due to their excellent performance^[1]. As a substrate protective layer, it must be ensured to remain intact during the service of the device in order to ensure the reliability of the device, equipment, etc^[2,3]. The harm of coating failure is enormous, and the most common forms of failure include cracking, peeling, delamination, etc. Research has shown that high residual stress is the main cause of coating bonding failure^[4,5]. The residual stress is usually closely related to the microstructure, which is determined by the characteristics of its preparation technology. Therefore, the microstructure and residual stress state of the coating determine its service performance^[6-8]. One of the common shortcomings of traditional magnetron sputtering and high power pulse

magnetron sputtering technology is that the residual stress of the prepared coating is high, which makes the coating prone to peeling and fracture during long-term service, seriously affecting its practical application in industrial engineering^[9,10].

Through in-depth analysis of the principles of high power pulsed magnetron sputtering (HIPIMS), it is known that using high power glow pulse discharge has a dual nature. The advantage is that high power pulsed glow discharge can be used to achieve high ionization deposition of the plating material, which can improve the microstructure of the coating and enhance the mechanical properties of the coating^[11]. The disadvantage is that according to the principle of high voltage induced atomic ionization, the generation of high-density plasma inevitably requires the use of extremely high voltage (nearly kilovolts) or extremely high power. On the one hand, it

makes the ionized plating material in the cathode sheath area of the target surface easily attracted by negative high voltage to return to the target surface, causing serious loss of the plating material. On the other hand, its discharge duty cycle is at a low efficiency level below 5%, which seriously affects the deposition rate of the coating^[12].

The research proposes the concept of a dual-stage high power pulsed electric field, which designs the electric field mode as a stepped dual-stage high power pulsed electric field that is weak first and then strong^[13], with a duty cycle of up to 10% to 100%. In the weak ionization stage, lower power causes Ar to undergo initial ionization, forming low-density plasma within the vacuum chamber. In the strong ionization stage, high power further ionizes atoms, forming high-density plasma. The pre ionization effect generated during the weak ionization stage can significantly reduce the voltage of the high-density plasma generated during the strong ionization stage, reduce the probability of the coated particles being returned to the target surface by the electric field, and avoid the loss of the coated material. In addition, pre ionization has a certain reducing effect on residual stress in the coating. With the significant increase of target current, the intensity and frequency of Ar⁺ bombardment on the target surface during the strong ionization stage increase significantly, and the collision ionization rate of the plating material and the deposition rate of the coating also increase significantly. The ultimate goal is to achieve both the performance goal of high ionization rate deposition of high power pulsed magnetron sputtering materials and the efficiency goal of high-speed deposition^[14,15].

This study utilized a novel dual stage HIPIMS technology to prepare TiN coatings under different deposition time conditions. The influence and mechanism of microstructure and stress state at different growth stages on the mechanical prop-

erties, tribological properties, and corrosion resistance of the coatings were analyzed. This is of great significance for evaluating the quality, service life, and practical application in the industrial field of the coatings.

1 Experiment

The experiment adopts a self-developed dual-stage high power pulse power supply system (peak power of 12 kW, duty cycle of 10%~100%), paired with MSIP-019 unbalanced closed field magnetron sputtering host equipment (vacuum chamber size of Φ 450 mm×H400 mm) for coating preparation. By changing the deposition time, TiN coatings were deposited on the surfaces of M2 high-speed steel sheets and monocrystalline silicon sheets, with a target substrate distance of 130 mm and a workpiece frame speed of 5 r/min. The detailed experimental parameters are shown in Table 1. The microstructure of the coating surface and cross-section was observed using SM-6700F scanning electron microscope and JEM-3010 transmission electron microscope. The three-dimensional morphology and roughness of the coating surface were characterized using the SPI3800-SPA-400 atomic force microscope. Using X-ray diffractometer $\sin^2\phi$ fit and calculate the residual stress of the coating. The hardness and Young's modulus of the coating samples were tested using the Nano Indenter G200 nanoindentation instrument. The friction and wear performance of the coating was tested using friction and wear testing machine. The Correst-CS350 electrochemical testing system was used to characterize the corrosion resistance of the coating. The polarization curve characteristics of the sample in 3.5 wt.% NaCl corrosive medium were measured by potentiodynamic scanning method, and the obtained polarization curve data was fitted using C-view software.

Table 1 Deposition parameters of TiN coatings deposited by dual-stage HIPIMS

Sample No.	I_p (A)	T_{on}' (ms)	T_{on}'' (ms)	T_{off} (ms)	U_t (V)	U_s (V)	N_2 (sccm)	Ar(sccm)	T_s (°C)	t(min)
1 [#]									50	30
2 [#]	2.2/20.0	2	4	8	220/525	-60	20	60	55	60
3 [#]									62	90
4 [#]									70	120

note: I_p —target peak current in the the weak and strong ionization phase, T_{on}' —The pulse conduction width in the weak ionization phase, T_{on}'' —The pulse conduction width in the strong ionization phase, T_{off} —Pulse turn-off width, U_t —target voltage in the weak and strong ionization phase, U_s —bias voltage, T_s —chamber temperature, t —deposited time

2 Results and Discussion

2.1 Microstructure

Fig.1 showed the surface microstructure morphology of TiN coatings deposited at different deposition times by dual-stage HIPIMS. As the deposition time continues to increase, the par-

ticle morphology on the surface of the coating presented a densely doped circular cell structure, with tight bonding between particles and no obvious defects. When the deposition time increased to 120 minutes, the coating still maintained the characteristics of circular cell growth, and these particles were tightly arranged together, showing a certain protrusion. Upon careful observation, it was found that these protrusions were

formed by the aggregation of several smaller clusters. The presence of these protrusions inevitably creates gaps, which slightly reduces the density of the coating, but the overall quality is good.

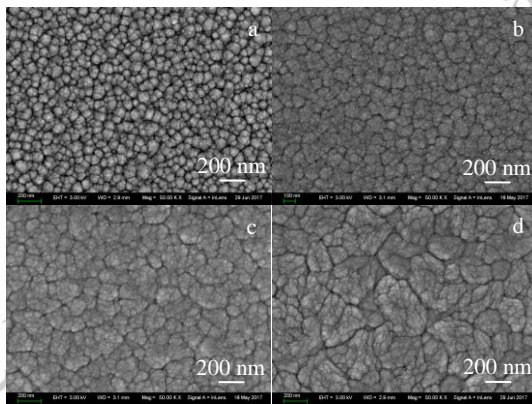


Fig.1 SEM images of surface (a) 30 minutes; (b) 60 minutes; (c) 90 minutes; (d) 120 minutes

The three-dimensional morphology and roughness R_a of TiN coating surface were detected using atomic force microscopy (AFM), with a selection range of $5 \times 5 \mu\text{m}^2$, as shown in Fig.2. There are significant differences in the AFM three-dimensional morphology and roughness of TiN coating surfaces under different deposition time conditions. When the deposition time is 30 minutes, the three-dimensional morphology of the coating surface presents sharp and small mountain peaks, with many grooves between peaks. The surface roughness of the coating is 16 nm. When the deposition time is 60 and 90 minutes, the three-dimensional morphology of the coating surface still shows a mountain peak shape, but the mountain peak structure gradually widens, indicating an increase in the average particle size of the coating surface. There are still obvious grooves between peaks, and the roughness slightly increases (R_a 22 and 27 nm). In summary, it indicates that during relatively short deposition times, the coating is mainly deposited in an island like manner with significant voids. As the deposition time continued to increase to 120 minutes, the surface of the coating exhibited a slightly larger sand dune like structure, with dense clusters and reduced gullies between the sand dune like structures. The surface roughness slightly increased (R_a 35 nm). Under the condition of dual pulse electric field, as the deposition time increases, the growth mode of the coating gradually changes from island like growth to island layered growth, and the surface of the deposited coating is relatively flat, with a maximum roughness of R_a 35 nm.

The crystal structure of the deposited coatings at 30 minutes and 120 minutes of deposition time were analyzed using high-resolution transmission electron microscopy. The high-resolution images and electron diffraction patterns of the selected area were shown in Figure 3. When the deposition time is 30 minutes, the degree of crystallization of the coating is low,

and the selected area electron diffraction pattern shows discontinuous multi round bright spots. When the deposition time is 120 minutes, the high-resolution image has complete lattice stripes in different lattice directions, with a large number and clear arrangement of lattice stripes. The selected area electron diffraction pattern shows a center symmetric multi circular bright ring. Used DM software to perform Fourier transform on selected areas of high-resolution film images. The calculated interplanar spacing is $d_{111}=0.245$ nm and $d_{110}=0.147$ nm, respectively. Corresponding to the lattice constants of TiN (111) and TiN (220) crystal planes, the crystal growth of the coating exhibits a typical polycrystalline structure. The growth process of the coating is closely related to the characteristics of the dual-stage pulse electric field and the deposition time. The strong ionization stage has the characteristic of instantaneous strong current, and the strong ionized particles have strong activity on the substrate surface, promoting the polycrystalline growth of the coating, thereby making the coating preferentially oriented along the polycrystalline plane direction. When the sedimentation time is short (30 minutes), the deposited particles do not have enough time to grow and diffuse, resulting in a lower degree of crystallization. With the increase of discharge time, the influence of electric field characteristics on the growth process of the coating increases. The coating material has three high characteristics, which can promote the optimal growth of polycrystalline planes in the coating.

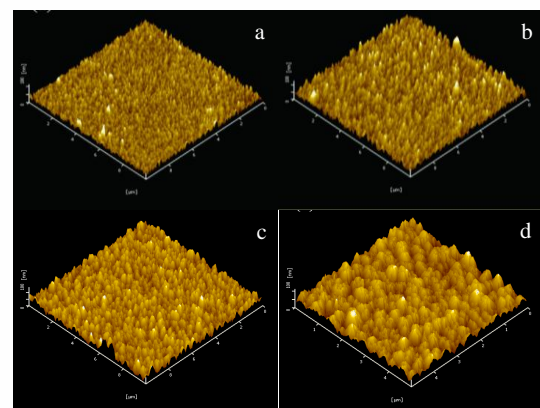


Fig.2 The AFM 3D morphologies of TiN coatings (a) 30 minutes; (b) 60 minutes; (c) 90 minutes; (d) 120 minutes

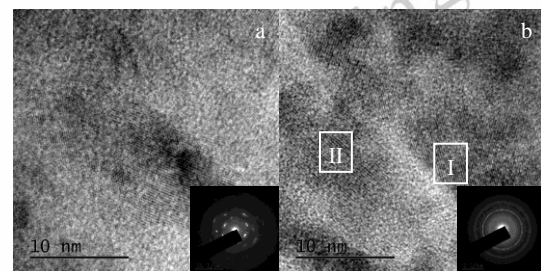
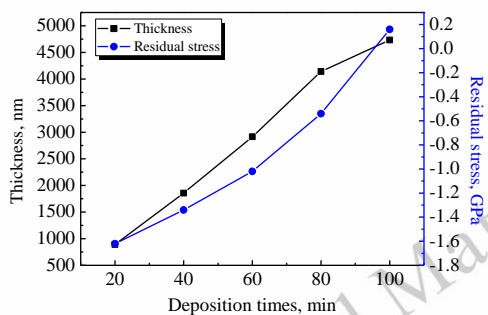


Fig.3 The TEM images and selected area electron diffraction patterns of TiN coatings (a) 30 minutes; (b) 120 minutes

2.2 Residual stress

Fig.4 showed the measurement results of the average thickness and residual stress of TiN coating. The thickness of the coating was 1220, 2535, 3884, and 4456 nm, respectively. When the deposition time increases from 30 minutes to 90 minutes, the coating thickness increases linearly with the increase of deposition time. When the deposition time continues to increase to 120 minutes, the film thickness increment significantly decreases. When the deposition time increased from 30 minutes to 90 minutes, the residual stress exhibited compressive stress. When the deposition time was 30 minutes, the highest compressive stress of the coating was about -1.62 GPa. When the deposition time increases to 90 minutes, the minimum compressive stress of the coating is about -0.54 GPa. When the sedimentation time continues to increase to 120 minutes, it is evident that residual stress transforms into tensile stress, which was about 0.16 GPa. As the deposition time increases, the residual stress of the coating changes from a compressive stress state to a tensile stress state, resulting in a compressive tensile transition phenomenon of the coating stress state, also known as the film thickness effect^[16].

Fig.4 The thickness and residual stress of TiN coatings



The residual stress changed during the growth process of the coating. The initial atomic shot peening effect during the growth of the coating under the action of a dual-stage pulse electric field is the main control mechanism for stress. The energetic particle flow composed of rebounding working gas atoms and sputtering atoms will generate significant compressive stress on the growth interface of the coating. As the deposition time increases, the atomic shot peening effect is not sufficient to continuously generate significant compressive stress during the growth process of the coating. When the coating grows to a certain extent, the recovery effect surpasses the atomic shot peening effect and occupies a dominant position. The deposition process of the coating is non-equilibrium, and the stress state is closely related to the microstructure of the coating. During the deposition process of the coating, the surface diffusion time obtained by the deposited atoms may not be long enough to keep them at the lattice position with the lowest energy, resulting in the formation of a metastable structure with a lower degree of order. During the reply process, the elimination of various point defects and surface defects, as well as the ordered arrangement of atoms, usually

accompanies the elimination of voids and defects, thereby promoting volume shrinkage and densification. This process also generates tensile stress, and thicker coatings often have more voids and defects. Therefore, when the coating exceeds a certain critical thickness, the recovery effect dominates.

2.3 Mechanical properties

The mechanical properties of TiN coatings are important indicators for measuring the service life of coatings^[19]. The experiment utilizes nanoindentation to characterize the hardness and elastic modulus of the thin film, with an indentation depth of 1/10 of the film thickness, and uses the multi-point averaging method for calculation. The result was shown in Fig.5. As the deposition time increases, the hardness and elastic modulus of TiN coatings show a trend of first increasing and then decreasing. The hardness and elastic modulus of the coating are the highest (27.5 GPa, 340.2 GPa) when the deposition time is 90 minutes. When the deposition time is 120 minutes, although the thickness of the coating is relatively large, there are some obvious defects such as protrusions and voids in the coating, which reduce the hardness and elastic modulus of the coating.

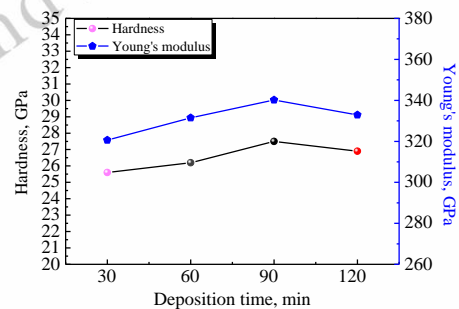


Fig.5 The hardness and Young's modulus of TiN coatings

2.4 Tribological properties

Fig.6 showed the instantaneous curve variation of the friction coefficient of TiN coatings prepared under different deposition times. The TiN coatings deposited at different deposition time conditions gradually enter a gentle stage after a brief running in period during the friction and wear process, and eventually reach a stable stage. The average value of the friction coefficient in the stable stage represents the friction coefficient^[20]. As the deposition time increases, the average friction coefficients of TiN coatings are 0.60, 0.56, 0.52, and 0.53, showing a trend of first decreasing and then slightly increasing. The sliding friction coefficient is mainly related to the characteristics of the coating material and surface roughness. There is no significant difference in surface roughness of the coating under different deposition times in this article, all of which are below 50 nm. Therefore, the characteristics of the coating material play a major determining role in the sliding friction coefficient, such as surface defects and crystal structure. The fewer surface defects, the more uniform the crystal structure, and the smaller the friction coefficient.

Fig.7 showed the mass wear rate of TiN coatings deposited at different deposition times after 30 minutes of wear experiment. When the deposition time is 90 minutes, the minimum wear rate of the coating is 1.68×10^{-4} g/s. When two objects in relative motion come into contact and friction occurs, the process of friction will inevitably cause wear and tear. The wear resistance of the coating during this experiment is mainly related to its hardness, thickness, and residual stress. The thicker the coating, the higher the hardness, and the presence of appropriate compressive stress, the longer the sliding distance it can withstand friction and wear, and the better its wear resistance.

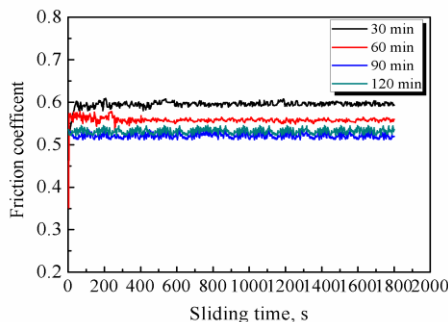


Fig.6 The curve of friction coefficient of TiN coatings

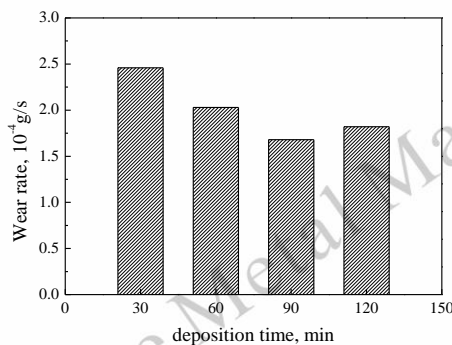


Fig.7 The wear ratio of TiN coatings

2.5 Corrosion resistance

The electrochemical polarization curve test results of TiN coatings deposited at different deposition times were shown in Figure 8. The electrochemical parameters of the polarization curve were fitted using C-View software to obtain the corrosion potential (E_{corr}), corrosion current density (I_{corr}), and corrosion rate (V_{corr}), as shown in Table 2.

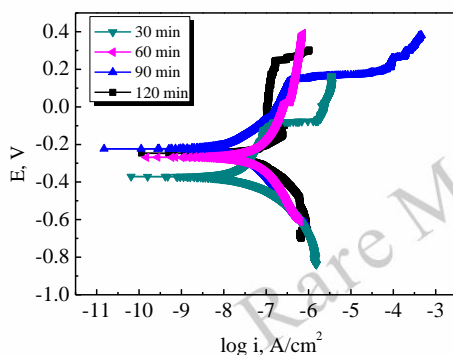


Fig.8 Electrochemical polarization curves of TiN coatings

As the deposition time increases, the corrosion current density and corrosion rate of TiN film show a trend of first decreasing and then slightly increasing. When the deposition time is 90 minutes, the corrosion current density and corrosion rate of TiN film are the smallest (1.0632×10^{-8} A cm^{-2} , 5.5226×10^{-5} mm A^{-1}). The corrosion resistance of the coating is the best. According to the corrosion mechanism of the coating, if there are defects such as micropores or voids in the coating structure, the corrosion solution will penetrate into the substrate through micropores and other defects under capillary force, forming a corrosion channel and causing corrosion to occur first at the interface between the coating and the substrate^[21,22]. During the corrosion process, hydrogen gas is continuously released due to hydrogen evolution reaction, which accumulates at the junction of the coating and substrate, generating high pressure, thereby intensifying the formation of pores and the peeling of the coating. The corrosion process was shown in Fig.9. Therefore, the corrosion resistance of the coating is closely related to its density and thickness^[23]. A coating with dense microstructure, fewer defects, and larger thickness can effectively block the contact, diffusion, and reaction between the corrosion solution and it, which helps to improve the corrosion resistance of the coating^[24,25]. Therefore, when the deposition time is 90 minutes, the corrosion resistance of the coating is optimal.

Table 2 Results of electrochemical tests in 3.5% NaCl solution

Deposition time(min)	E_{corr} (V)	I_{corr} (A cm^{-2})	V_{corr} (mm A^{-1})
30	-0.37582	2.0689×10^{-8}	1.3344×10^{-4}
60	-0.32830	1.1405×10^{-8}	1.0831×10^{-4}
90	-0.22435	1.0632×10^{-8}	5.5226×10^{-5}
120	-0.24113	1.1354×10^{-8}	5.9217×10^{-5}

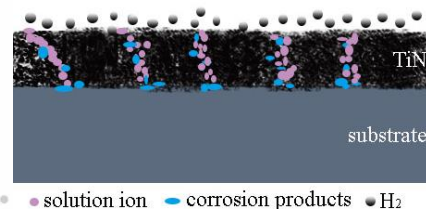


Fig.9 The schematic diagram of corrosion mechanism of TiN coatings

3 Conclusions

1) As the thickness of the coating increases, the surface structure of TiN coating shows a round cell structure with tightly doped particles of different sizes, maintaining the

atomic stacking thickening mechanism of deposition crystallization growth.

2) As the deposition time increases from 30 minutes to 90 minutes, the residual stress of the coating shows a compressive stress state, and as the deposition time increases, the compressive stress gradually decreases. When the deposition time continues to increase to 120 minutes, the residual stress state of the coating undergoes a compressive tensile transition, which is mainly caused by the change in the stress dominant mechanism during the deposition process of the coating.

3) When the deposition time is 90 minutes (3884 nm), the coating has the highest hardness value, good tribological and corrosion resistance, indicating that a dense structure and low compressive stress are beneficial for improving the service performance of the coating.

References

- 1 R Yavorskyi, L Nykyryu, G Wisz et al. Applied Nanoscience[J], 2019, 9 (5): 715-724
- 2 WJL A, EYY A, HBRL B et al. Applied Surface Science[J], 2020, 519, 146215: 1-4
- 3 Gao C, Wang Z, Xiao Z et al. Journal of Materials Processing Technology[J], 2020, 281, 116618:1-5
- 4 M. Meindlhumer, N. Jäger, S. Spor et al. Scripta Materialia[J], 2020, 182: 11-15
- 5 DH Kuo, KW Huang. Surface & Coating Technology[J], 2001, 135:150-157
- 6 X Du, B Gao, Y Li et al. Applied Surface Science[J], 2020, 511, 145653: 1-4
- 7 Y Wang, Y Gao, J Takahashi et al. Vacuum[J], 2019, 168, 108829, 1-4
- 8 Du Xiaoye, Gao Bo, Li Yanhui, Song et al. Journal of Alloys and Compounds[J], 2020, 812, 152140: 1-5
- 9 Q Zhang, Z Wu, Y Xu et al. Surface & Coatings Technology[J], 2019, 378, 125002: 1-4
- 10 HD Mejia, AM Echavarría, JA Calderon et al. Journal of Alloys and Compounds[J], 2020, 828, 154396: 1-3
- 11 J Lin, JJ Moore, WD Sproul et al. Surface & Coatings Technology[J], 2010, 204: 2230-2239
- 12 A Anders. Applied Physics Letters[J], 2014, 105: 244104-3
- 13 Yang Chao, Wang Rong, Jiang Bailing et al. Ceramics International[J], 2022, 20(48): 29652-29658
- 14 Wang Rong, Yang Chao, Hao Juan et al. Coatings[J], 2022, 12(3): 394
- 15 Yang Chao, Hao Juan, Jiang Bailing et al. Rare Metal Materials and Engineering[J], 2022, 9(51): 3276-3281
- 16 Koller CM, Marihart H, Bolvardi H et al. Surface & Coatings Technology[J], 2018, 347: 304-312
- 17 Ding J, Yin X, Fang L et al. Materials[J], 2018, 11, 1400: 1-4
- 18 DL Ma, PP Jing, YL Gong et al. Vacuum[J], 2019, 160: 226-232
- 19 JH Huang, KJ Yu, P Sit et al. Surface and Coatings Technology[J], 2006, 200: 4291-4299
- 20 YXC Fu. Ceramics International[J], 2020, 15(46): 24302-24311
- 21 JM Gonzalez-Carmona, JD Trivino, A Gomez-Ovalle et al. Ceramics International[J], 2020, 15(46): 24592-24604
- 22 MCH Wang. Surface & Coatings Technology[J], 2020, 391, 125660: 1-5
- 23 A Awan, RA Pasha, MS Butt et al. Journal of Mechanical Science and Technology[J], 2020, 8(34): 3227-3233
- 24 L Wang, M Wang, H Chen. Corrosion[J], 2020, 7(76): 628-638
- 25 Raynald Guilbault, Sébastien Lalonde. Tribology International[J], 2019, 140, 105854: 1-4

微观结构与应力状态对双级 HIPIMS 沉积 TiN 镀层服役性能的影响

郝娟^{1,2}, 王百川¹, 丁郁航¹, 杨超¹, 蒋百灵¹, 王梓毅¹, 汪东城²

(1. 西安理工大学材料科学与工程学院, 陕西 西安 710048)

(2. 嘉善鑫海精密铸件有限公司, 浙江 嘉善 314105)

摘要：研究利用新型双级 HIPIMS 技术在不同沉积时间条件下制备得到 TiN 镀层，分析不同镀层生长阶段其微观结构与应力状态对镀层力学、摩擦学、耐腐蚀等服役性能的影响。结果表明，随着沉积时间由 30min 增加至 120min，TiN 镀层表面结构均呈大小颗粒紧密掺杂的圆胞状结构，始终保持沉积-结晶-生长的原子堆积增厚机制，当沉积时间由 90min（镀层厚度 3884nm）增加至 120min（镀层厚度 4456nm）时，镀层应力状态出现压-拉转变。当沉积时间为 90min 时，TiN 镀层结构致密且较小的压应力（-0.54 GPa），镀层具有较高的硬度与弹性模量（27.5 GPa、340.2 GPa）、较好的摩擦学性能（平均摩擦系数 0.52，最小磨损率 1.68×10^{-4} g/s）及耐腐蚀性能（最小腐蚀电流密度 1.0632×10^{-8} A cm^{-2} 、最小腐蚀速率 5.5226×10^{-5} mm A^{-1} ）。

关键词：双级HIPIMS; TiN镀层; 应力; 服役性能

作者简介：郝娟，女，1990 年生，博士，讲师，西安理工大学材料科学与工程学院，陕西 西安 710048，电话：029-82312812，
E-mail:haojuan19901207@163.com